

## A phase I study of $^{99m}\text{Tc}$ -hR3 (DiaCIM<sup>®</sup>), a humanized immunoconjugate directed towards the epidermal growth factor receptor

K.A. VALLIS,<sup>1,7,\*</sup> R.M. REILLY,<sup>3,8,9</sup> P. CHEN,<sup>3</sup> A. OZA,<sup>2</sup> A. HENDLER,<sup>3,8</sup>  
R. CAMERON,<sup>4</sup> M. HERSHKOP,<sup>3,8</sup> N. IZNAGA-ESCOBAR,<sup>5</sup> M. RAMOS-SUZARTE<sup>5</sup>  
and P. KEANE<sup>6</sup>

Departments of <sup>1</sup>Radiation Oncology and <sup>2</sup>Medical Oncology, The Princess Margaret Hospital, Toronto, Canada; <sup>3</sup>Division of Nuclear Medicine and <sup>4</sup>Department of Pathology, Toronto General Hospital, University Health Network, Toronto, Canada; <sup>5</sup>Center of Molecular Immunology, Havana, Cuba; <sup>6</sup>YM Biosciences Inc., Mississauga, Ontario, Canada; and Departments of <sup>7</sup>Medical Biophysics, <sup>8</sup>Medical Imaging and <sup>9</sup>Pharmaceutical Sciences, University of Toronto, Toronto, Canada

Received 17 April 2002 and accepted 17 July 2002

### Summary

A phase I trial was conducted to evaluate the safety, tumour and normal tissue localization, pharmacokinetics and radiation dosimetry of  $^{99m}\text{Tc}$ -hR3, a humanized monoclonal antibody directed towards the epidermal growth factor receptor, in 12 patients with recurrent or metastatic epithelial malignancies. Patients were injected intravenously with 3.0 mg or 6.0 mg (1010 MBq) of  $^{99m}\text{Tc}$ -hR3. Blood and plasma concentrations of radioactivity were measured and a complete 24 h urine collection was obtained. Whole-body images were acquired up to 24 h post-injection and normal organ uptake quantified. Radiation dosimetry was estimated using MIRDose. Safety was evaluated by clinical observation, biochemical/haematological testing and by measuring immune response to  $^{99m}\text{Tc}$ -hR3. There were no adverse effects, no changes in biochemical/haematological indices and no immune response to  $^{99m}\text{Tc}$ -hR3.  $^{99m}\text{Tc}$ -hR3 was rapidly cleared from the blood with a distribution half-life of  $10.8 \pm 3.8$  min. The volume of distribution,  $V_d$ , and clearance,  $C$ , were  $180 \pm 37$  ml·kg<sup>-1</sup> and  $14 \pm 3$  ml·kg<sup>-1</sup>·min<sup>-1</sup>, respectively. The elimination phase could not be discerned due to increasing blood radioactivity at later times. About 19–24% was excreted in the urine. Normal tissue uptake was mainly in the liver (44–50%), spleen (3–4%) and kidneys (3%). Imaging was positive in one patient with squamous cell carcinoma of the mouth and an involved cervical lymph node. The whole-body radiation dose from  $^{99m}\text{Tc}$ -hR3 was  $1.34 \pm 0.02 \times 10^{-8}$  mSv·Bq<sup>-1</sup>. We conclude that  $^{99m}\text{Tc}$ -hR3 exhibited an excellent safety profile. Future studies to determine the sensitivity and specificity of imaging with  $^{99m}\text{Tc}$ -hR3 in a larger group of patients with pre-selection for epidermal growth factor receptor positivity are planned. (© 2002 Lippincott Williams & Wilkins)

**Keywords:** epidermal growth factor receptor, monoclonal antibody, pharmacokinetics, safety, imaging.

### Introduction

Overexpression of cell surface receptors for peptide growth factors represents an appealing target for the

design of new molecular imaging agents for cancer [1]. One candidate peptide growth factor receptor is the epidermal growth factor receptor (EGFR), a 170 kDa transmembrane receptor tyrosine kinase which specifically binds epidermal growth factor (EGF) and transforming growth factor- $\alpha$  (TGF $\alpha$ ). Overexpression of EGFR has been observed in breast cancer, colorectal cancer, ovarian cancer, squamous cell lung carcinoma, head and neck cancer and bladder cancer [2]. Molecular imaging using radiopharmaceuticals directed towards EGFR

\*Address all correspondence to Dr Katherine A. Vallis, Department of Radiation Oncology, Princess Margaret Hospital, 610 University Avenue, Toronto, Ontario, Canada M5G 2M9.  
e-mail: katherine.vallis@rmp.uhn.on.ca

could characterize the receptor status of tumours and thereby predict response to novel anti-EGFR agents currently under development for the treatment of malignancies. Novel therapeutic agents directed towards EGFR overexpression include specific tyrosine kinase inhibitors such as Iressa<sup>®</sup> (ZD1839) [3], anti-EGFR monoclonal antibodies (e.g. mAb C225) [4], EGF or TGF $\alpha$  toxin fusion proteins [5, 6], as well as targeted radio-therapeutic agents (e.g. <sup>111</sup>In-EGF) [7].

mAb ior egf/r3 is a murine IgG<sub>2a</sub> antibody that specifically recognizes an epitope on the extracellular domain of the EGFR with high affinity ( $K_a = 10^9 - 10^{10}$  l·mol<sup>-1</sup>) and inhibits the binding of EGF to its receptor [8]. In phase I/II testing, <sup>99m</sup>Tc-mAb ior egf/r3 imaged a diverse group of tumours of epithelial origin, with a sensitivity ranging from 74% for head and neck cancers to 100% for brain tumours, with overall specificity of 100% [9]. The clinical utility of <sup>99m</sup>Tc-mAb ior egf/r3 for tumour imaging is limited, however, by its immunogenicity [9]. This is particularly problematic if repeat imaging studies are required. The mAb hR3 is a humanized form of mAb ior egf/r3. It was constructed by grafting the complementarity determining regions (CDRs) of the murine antibody onto a human IgG<sub>1</sub> framework [10]. CDR grafting diminished the receptor binding affinity of the antibody, but a variant in which three murine residues were retained (Ser-75, Thr-76 and Thr-93) exhibited a similar affinity as the original murine mAb ( $K_a = 1 \times 10^9$  l·mol<sup>-1</sup>) [10]. In this study, we conducted a phase I trial to evaluate the safety of administration of <sup>99m</sup>Tc-hR3 to humans, its pharmacokinetics, normal tissue biodistribution, and radiation dosimetry as well as to obtain a preliminary assessment of its tumour localization properties.

## Patients, materials and methods

### Patients

Twelve eligible patients with histologically proven epithelial derived carcinomas were enrolled in the study. Eligibility criteria were: age between 18 and 80 years, radiological or clinical evidence of recurrent or metastatic cancer, WHO performance status of 0–2, leukocyte count  $\geq 4 \times 10^9$ /l, platelets  $\geq 100 \times 10^9$ /l and haemoglobin  $\geq 10$  g·dl<sup>-1</sup>. The following clinical biochemistry indices were required to be within normal limits: alanine transaminase (ALT), aspartate transaminase (AST), alkaline phosphatase, total protein, albumin, bilirubin, glucose, cholesterol, triglycerides, urea, creatinine and electrolytes. Patients were ineligible if they had received chemotherapy during the preceding 4 weeks. Tumour EGFR positivity was not an entry criterion for the study. All patients gave written informed consent to take part in

the study which was approved by the Human Subjects Review Committee, University of Toronto. Patients' characteristics are summarized in Table 1.

### Radiopharmaceutical preparation and quality control

Unit dose kits of hR3 suitable for labelling with <sup>99m</sup>Tc were manufactured by the Center for Immunology (CIM), Havana, Cuba and supplied by YM Biosciences, Inc. (Mississauga, Ontario, Canada). Each lyophilized kit contained 3.0 mg of mercaptoethanol-reduced hR3, 190  $\mu$ g methylene diphosphonate (MDP), 10.2  $\mu$ g stannous fluoride, 60  $\mu$ g *p*-aminobenzoate and 15 mg of glucose in a sterile, apyrogenic sodium phosphate/sodium chloride buffer. <sup>99m</sup>Tc-hR3 was prepared by reconstituting a kit with 1.5–3.0 ml (555–1110 MBq, 15–30 mCi) of sodium [<sup>99m</sup>Tc]pertechnetate freshly eluted from a <sup>99</sup>Mo/<sup>99m</sup>Tc generator (Dupont Pharma, North Billerica, MA) and incubating the reconstituted kit for 15 min at room temperature. The radiochemical purity of <sup>99m</sup>Tc-hR3 was measured by instant thin layer silica gel chromatography (ITLC-SG, Gelman, Ann Arbor, MI) using three different systems. In system 1, ITLC-SG strips were developed in acetone to determine the percentage of free <sup>99m</sup>Tc ( $R_f = 1.0$ ). In system 2, ITLC-SG strips were developed in 0.9% sodium chloride to determine the combined percentage of <sup>99m</sup>Tc-MDP and free reduced-hydrolysed <sup>99m</sup>Tc ( $R_f = 0.0$ ) impurities. In system 3, ITLC-SG strips pre-saturated with 1% bovine serum albumin were developed in a 1:2:5 mixture of ammonium hydroxide/ethanol/water to determine the percentage of free reduced-hydrolysed <sup>99m</sup>Tc ( $R_f = 0.0$ ). The percentage of <sup>99m</sup>Tc-MDP impurity was obtained by subtraction of the proportion of free reduced-hydrolysed <sup>99m</sup>Tc from the combined impurities determined in system 2.

### Radiopharmaceutical administration and safety evaluation

<sup>99m</sup>Tc-hR3 was administered by slow intravenous injection over 2–3 min. The first six patients enrolled in the study received 3.0 mg (approx. 1010 MBq, 27 mCi) of <sup>99m</sup>Tc-hR3 and the next six patients received 6.0 mg (approx. 1010 MBq, 27 mCi) of <sup>99m</sup>Tc-hR3. Vital signs were recorded prior to administration of the radiopharmaceutical and at 10 min, 1 h and 24 h after administration and any adverse effects recorded. Blood samples were collected prior to <sup>99m</sup>Tc-hR3 injection, and at 24 and 48 h after injection for haematology and clinical biochemistry analyses. Toxicity was graded as 0 to 4 according to the WHO classification. Serum samples obtained prior to administration and at 2 weeks and 4–5 weeks after administration of the radiopharmaceutical were assayed for human anti-human antibodies (HAHA) and human anti-mouse antibodies (HAMA) using an

Table 1. Patient's characteristics.

Patient number	Age (years)	Gender	Primary tumour/histology	Metastases	<sup>99m</sup> Tc-hR3 (mg:MBq <sup>-1</sup> )	Tumour immuno-histochemistry score		
						Positive cells*	Intensity†	Tumour imaging
1	68	F	Breast/ovary (mixed invasive ductal/lobular carcinoma)	Peritoneum	3.0/884	4	4	FN
2	59	F	Breast (infiltrating ductal carcinoma)	Bone	3.0/894	n.d.‡	n.d.	FN
3	74	F	Breast (infiltrating ductal carcinoma)	Mediastinal LN, bone	3.0/1208	n.d.	n.d.	FN
4	45	F	Breast (infiltrating ductal carcinoma)	Bone	3.0/989	1	1	FN
5	65	M	Floor of mouth (squamous cell carcinoma)	Cervical LN	3.0/938	5	4	TP
6	80	F	Breast (infiltrating ductal carcinoma)	Bone	3.0/974	n.d.	n.d.	FN
7	64	M	Lung cancer (adenocarcinoma)	Mediastinal LN	6.0/703	3	2	FN
8	78	F	Supraglottic laryngeal (squamous cell carcinoma)	Lung	6.0/902	4	3	FN
9	76	M	Prostate (adenocarcinoma)	Bone, paraaortic LN	6.0/1006	n.d.	n.d.	FN
10	51	M	Skin, parotid (basal squamous cell carcinoma)	Lung, bone	6.0/1004	5	4	FN
11	46	M	Ascending colon (mucinous adenocarcinoma)	Bone	6.0/970	1	1	FN
12	53	M	Lung (non-small cell cancer)	Mediastinal LN, adrenals	6.0/1010	5	4	FN

\*Proportion of malignant cells in primary tumour biopsy staining with anti-EGFR mAb (31G7, Zymed Lab Inc.) on a scale of 0 (no staining) to 5+ (>90% of cells staining).

†Intensity of staining of malignant cells in primary tumour using anti-EGFR mAb (31G7, Zymed Lab Inc.) on a scale of 0 (no staining) to 4+ (strong staining).

‡n.d.: Not determined due to unavailability of primary tumour biopsy specimen.

FN, false negative; TP, true positive; LN, lymph nodes.

ELISA assay. For measurement of HAHA, serum samples were diluted 1:50 to 1:100 in phosphate buffered saline (PBS)/0.05% Tween 20 and incubated in wells on a microELISA plate pre-coated with Fab' fragments of hR3 for 1 h at 37°C. The plates were rinsed three times with PBS/0.05% Tween 20, then incubated with anti-human IgG and anti-human IgM antibodies conjugated to alkaline phosphatase for 1 h at 37°C. The plates were rinsed three times with PBS/0.05% Tween 20 and incubated with 1 mg·ml<sup>-1</sup> *p*-nitrophenylphosphate in diethanolamine buffer pH 9.8 for 30 min at room temperature in the dark. The absorbance of the wells was measured at 405 nm using a plate reader. The HAMA assay was identical except that the microELISA plates were precoated with murine mAb ior-r/3. A positive immune response was defined as an absorbance which was more than 2-fold higher than that obtained for a serum sample obtained prior to administration of <sup>99m</sup>Tc-hR3.

#### Pharmacokinetic analysis

Blood samples were obtained in heparinized Vacutainer<sup>®</sup> tubes at 5, 10, 15, 20, 30 min and at 1, 3, 5 and 24 h post-injection of <sup>99m</sup>Tc-hR3 for pharmacokinetic analysis. Blood samples were centrifuged at 500 × *g* for 10 min to obtain plasma and 200 μl of whole blood or plasma was dispensed into gamma-counting tubes and counted along with a sample of injected radiopharmaceutical in an automatic gamma counter (Packard Cobra Quantum, Meriden, CT) for 1 min using a window (130–150 keV) to include the 140 keV γ-photon of <sup>99m</sup>Tc. A complete 24 h urine collection was also obtained. The total volume of urine was measured and a 1.0 ml sample counted in the gamma counter for <sup>99m</sup>Tc. The concentration of <sup>99m</sup>Tc in the blood and plasma (cpm/ml) was decay corrected to the time of injection and plotted against the time post-injection of <sup>99m</sup>Tc-hR3. Decay correction was performed to evaluate the pharmacokinetics of <sup>99m</sup>Tc-hR3 independent of the physical decay of the radionuclide. The total amount of <sup>99m</sup>Tc excreted in the urine in 24 h (per cent injected dose, %ID) was calculated. Pharmacokinetic data were fitted to a one-compartment pharmacokinetic model using GraphPad Prism<sup>®</sup> software and standard pharmacokinetic parameters were calculated (distribution half-life (*T*), volume of distribution (*V<sub>d</sub>*), clearance (*C*) and mean residence time (MRT)).

#### Imaging studies

Patients were imaged at 30 min and at 1, 3, 5 and 24 h after administration of <sup>99m</sup>Tc-hR3. Anterior and posterior whole-body planar images were obtained on a General Electric Maxxus gamma camera fitted with a low energy

all-purpose (LEAP) collimator and interfaced to a Genie 4000i computer. SPECT images were obtained at 3–5 h after injection of  $^{99m}\text{Tc}$ -hR3. Regions of interest (ROIs) were drawn around the heart, liver, spleen, kidneys, gastrointestinal tract, thyroid and the whole body. The total cpm was obtained for each ROI at the selected imaging time points. It was assumed that the whole-body counts immediately after injection of the radiopharmaceutical represented 100% of the injected dose. The percentage of the injected dose in each organ at each time point was obtained by dividing the ROI counts (corrected for decay from the time of injection) by the whole-body counts.

#### *Radiation dosimetry estimates*

Prior to administration of the radiopharmaceutical, the syringe containing the dose of  $^{99m}\text{Tc}$ -hR3 was assayed in a radioisotope calibrator (Capintec CRC-12, Montvale, NJ) and then placed directly on the collimator of the gamma camera and imaged for 1 min to determine the relationship between cpm by imaging and the assay value (kBq). The radioactivity contained in each organ (kBq) at selected imaging time points was calculated from ROI analysis using the cpm/kBq relationship. The mean residence time for  $^{99m}\text{Tc}$  ( $\tau$ , h) in each organ was calculated by integrating the radioactivity versus time curve and dividing the area under the curve (kBq  $\times$  h) by the injected dose (kBq). Radiation dosimetry estimates were calculated using the MIRDOSE computer program [11] as  $\bar{D} = \tau S$ , where  $S$  is the mean absorbed radiation dose to a target organ per unit cumulated radioactivity in the source organ.

#### *Immunocytochemical staining of tumours*

EGFR expression of primary tumour biopsies when available was evaluated retrospectively (not as an entry criterion). Archival paraffin embedded blocks of primary tumour biopsies were obtained. Sections (3  $\mu\text{m}$ ) were cut, de-waxed in toluene and rehydrated through graded alcohol to water. Endogenous peroxidase activity was blocked in 3% hydrogen peroxide. After pretreatment in pepsin, slides were incubated in primary antibody for 1 h at room temperature. The primary antibody, anti-EGFR murine mAb (31G7, Zymed Lab. Inc., San Francisco, CA), was used at 1:50 dilution. Following washing in phosphate buffered saline, secondary incubations were carried out with biotin conjugated multi-link IgG (Signet Pathology Systems Inc., Dedham, MA) followed with streptavidin–horse radish peroxidase (HRP) incubation in 3-amino-9-ethylcarbazol (AEC). Slides were counterstained in haematoxylin and mounted with crystal mount. The slides were reviewed and the proportion of EGFR positive

cells scored on a scale of 0 to 5 as follows: 0 (no staining), 1 (<10% of cells staining), 2 (10–25% staining), 3 (25–50% staining), 4 (50–75% staining) or 5 (>75% of cells staining). Similarly, the intensity of EGFR staining was qualitatively scored from 0 (no staining) to 4 (strong staining).

#### *Statistical comparisons*

Statistical comparisons were performed using Student's  $t$  test ( $P < 0.05$ ).

## **Results**

#### *Radiopharmaceutical preparation and quality control*

The mean labelling efficiency for  $^{99m}\text{Tc}$ -hR3 kits was  $92.8 \pm 3.2\%$  ( $n = 18$ ). The mean percentage of free  $^{99m}\text{Tc}$  pertechnetate,  $^{99m}\text{Tc}$ -MDP and free, reduced-hydrolysed  $^{99m}\text{Tc}$  impurities was  $2.4 \pm 2.7\%$ ,  $2.8 \pm 2.9\%$  and  $1.1 \pm 1.0\%$ , respectively.

#### *Radiopharmaceutical administration and safety evaluation*

No adverse reactions or side effects were observed following the administration of  $^{99m}\text{Tc}$ -hR3. Peripheral blood counts and clinical biochemistry remained within the normal range. No clinically significant changes in bone marrow, liver or kidney function were observed in any of the patients. There was no significant increase in HAHA up to 16 days post-injection of  $^{99m}\text{Tc}$ -hR3 or HAMA serum levels up to 37 days post-injection in the first six patients who were administered 3.0 mg of  $^{99m}\text{Tc}$ -hR3. The mean absorbance for pre-injection serum samples in the HAHA assay was  $0.30 \pm 0.11$  and in samples obtained 2 weeks after injection of  $^{99m}\text{Tc}$ -hR3 was  $0.31 \pm 0.08$  (mean ratio of pre/post-injection absorbance values  $1.07 \pm 0.31$ ). The mean absorbance of pre-injection serum samples in the HAMA assay was  $0.42 \pm 0.07$ , in samples obtained 2 weeks after injection of  $^{99m}\text{Tc}$ -hR3 was  $0.55 \pm 0.11$  (mean ratio of pre/post-injection absorbance values  $1.33 \pm 0.12$ ) and in samples obtained 4–5 weeks after injection was  $0.54 \pm 0.10$  (mean ratio of pre/post-injection absorbance values  $1.35 \pm 0.10$ ). Immune response was not measured in the second six patients who received 6.0 mg of  $^{99m}\text{Tc}$ -hR3.

#### *Pharmacokinetic analysis*

$^{99m}\text{Tc}$ -hR3 exhibited a rapid elimination from the blood and plasma within 1 h (distribution phase) which was followed by an increase in circulating  $^{99m}\text{Tc}$  radioactivity (corrected for decay) over a 24 h period (Fig. 1). Sufficient data points for pharmacokinetic analysis of the distribu-

tion phase were available for five of 12 patients (Table 2). In these patients, the mean distribution half-life was  $10.8 \pm 3.8$  min, the  $V_d$  was  $180.7 \pm 36.7$   $\text{ml}\cdot\text{kg}^{-1}$  and the clearance was  $13.9 \pm 3.0$   $\text{ml}\cdot\text{kg}^{-1}\cdot\text{min}^{-1}$ . The elimination phase of  $^{99m}\text{Tc}$ -hR3 could not be discerned due to the increase in circulating radioactivity in all patients at later time points. The concentration of  $^{99m}\text{Tc}$  in the blood or

plasma increased 3- to 4-fold at 24 h compared to those measured at 1 h post-injection. The mean cumulative excretion of  $^{99m}\text{Tc}$  into the urine over 24 h for all 12 patients was  $21.7 \pm 3.8\%$ ID. There was no significant difference in urinary excretion of  $^{99m}\text{Tc}$  between patients administered 3.0 mg or 6.0 mg of  $^{99m}\text{Tc}$ -hR3 ( $24.0 \pm 3.3$  vs  $19.3 \pm 4.2\%$ ID, respectively).

#### Imaging studies

The heart and blood pool was observed on images acquired immediately after injection of  $^{99m}\text{Tc}$ -hR3 in all patients. ROI analysis of the images revealed that the radiopharmaceutical accumulated mainly in the liver and to a lesser extent in the kidneys and spleen (Tables 3 and 4). There were no significant differences in liver uptake following a 3.0 mg or 6.0 mg dose ( $49.6 \pm 3.5$  vs  $44.0 \pm 2.2$  %ID/organ, respectively). Liver uptake declined more than 2-fold over a 24 h period. There were no significant differences between the 3.0 mg or 6.0 mg dose in kidney uptake at 5–10 min post-injection of the radiopharmaceutical ( $2.7 \pm 0.4$  vs  $3.2 \pm 0.3$  %ID/organ respectively) or in initial spleen uptake ( $3.2 \pm 0.4$  vs  $3.7 \pm 0.4\%$ ID/organ, respectively). Radioactivity in the kidneys increased 3-fold at 24 h. Slight urinary bladder radioactivity was observed on the 1 h images, but this was more prominent at 24 h. Similarly, intestinal radioactivity was low immediately after injection of  $^{99m}\text{Tc}$ -hR3 (2–3%ID/organ) but increased 3- to 4-fold at 24 h post-injection (Tables 3 and 4). Loops of small bowel were observed on images at 3–5 h and radioactivity was observed in the large intestine at 24 h.

Tumour was imaged in Patient 5. This patient had a squamous cell carcinoma of the floor of the mouth and scans showed uptake of radioactivity in the primary lesion and in an involved cervical lymph node at 3–5 h post-injection of  $^{99m}\text{Tc}$ -hR3 (Fig. 2). The original tumour biopsy specimens of this patient exhibited a high proportion of EGFR positive cells by immunocytochemical staining (score 4–5 on a scale of 0 to 5). The intensity of staining was also high (4 on a scale of 0 to 4). Another

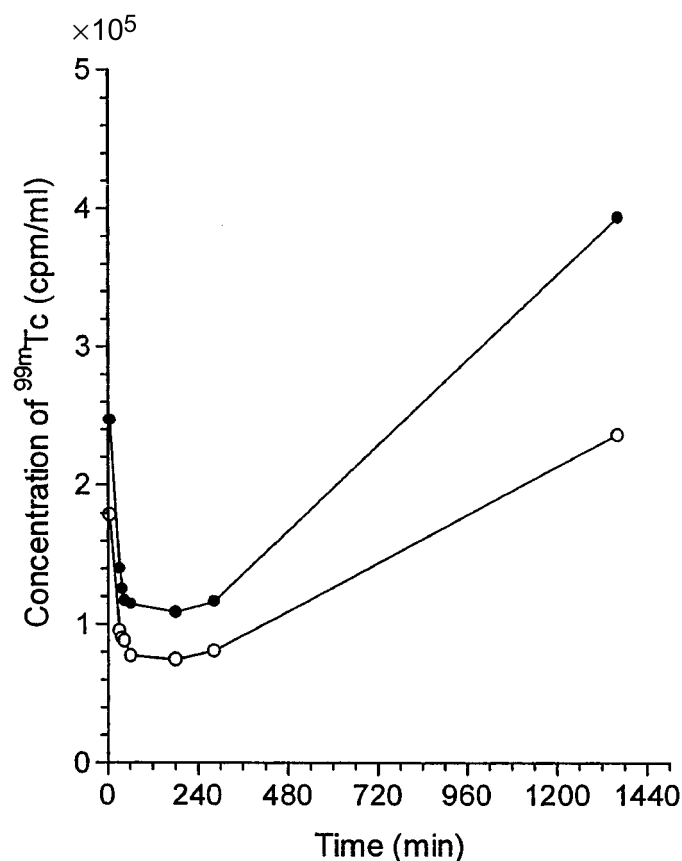


Fig. 1. Pharmacokinetics of  $^{99m}\text{Tc}$  radioactivity (corrected for decay) in the blood and plasma of a representative patient (Patient 9) administered  $^{99m}\text{Tc}$ -hR3 (6.0 mg, 1006 MBq). (●), Plasma; (○), blood.

Table 2. Pharmacokinetic analysis of distribution phase of  $^{99m}\text{Tc}$ -hR3.

Patient number	Dose of $^{99m}\text{Tc}$ -hR3 (mg·MBq <sup>-1</sup> )	$T_{1/2\alpha}$ (min)	$V_d$ (ml·kg <sup>-1</sup> )	Clearance (ml·kg <sup>-1</sup> ·min <sup>-1</sup> )	Mean residence time (min)
5	3.0/884	7.5	192.0	17.8	10.8
6	3.0/894	7.8	70.1	6.2	11.2
7	6.0/703	25.8	300.0	8.1	37.1
9	6.0/1006	7.5	163.5	15.0	10.8
12	6.0/1010	5.5	177.7	22.4	7.9
Mean ± SEM		$10.8 \pm 3.8$	$180.7 \pm 36.7$	$13.9 \pm 3.0$	$15.6 \pm 5.4$

$T_{1/2\alpha}$ , distribution half-life;  $V_d$ , volume of distribution.

**Table 3.** Pharmacokinetics of normal organ uptake of  $^{99m}\text{Tc}$ -hR3 following a 3 mg dose (1110 MBq). Results are given as per cent injected dose/organ (mean  $\pm$  SEM).\*

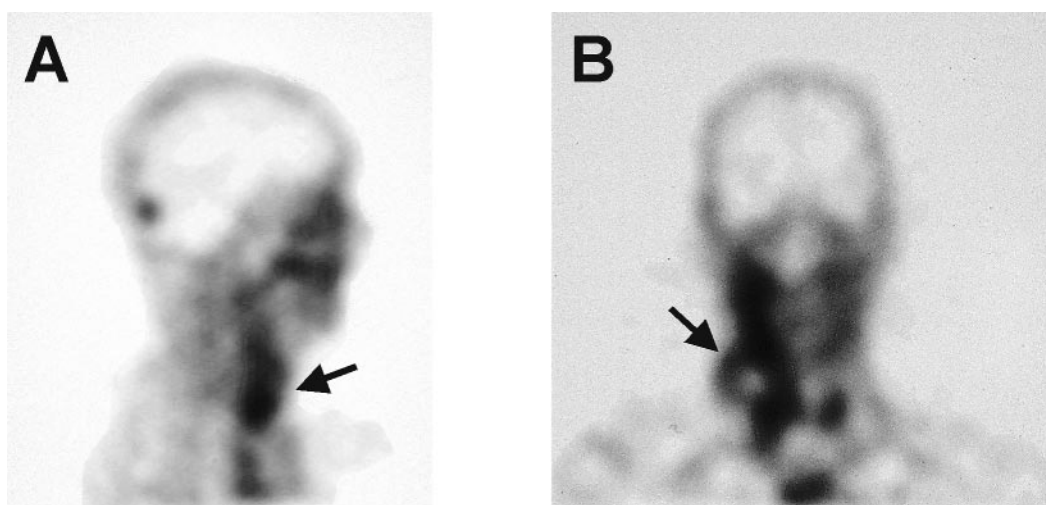
Organ	Time post-injection				
	5–10 min	1–2 h	2–4 h	4–6 h	24 h
Heart	4.1 $\pm$ 0.6	3.0 $\pm$ 0.4	2.5 $\pm$ 0.3	2.3 $\pm$ 0.3	1.3 $\pm$ 0.2
Liver	49.6 $\pm$ 3.5	52.9 $\pm$ 3.8	40.0 $\pm$ 1.5	36.7 $\pm$ 3.2	20.9 $\pm$ 2.0
Kidneys	2.7 $\pm$ 0.4	2.9 $\pm$ 0.3	4.8 $\pm$ 0.5	5.9 $\pm$ 0.4	10.1 $\pm$ 1.3
Spleen	3.2 $\pm$ 0.4	2.6 $\pm$ 0.3	2.1 $\pm$ 0.2	1.9 $\pm$ 0.2	1.6 $\pm$ 0.3
Thyroid	0.20 $\pm$ 0.03	0.17 $\pm$ 0.03	0.17 $\pm$ 0.03	0.17 $\pm$ 0.03	0.13 $\pm$ 0.03
Gastrointestinal tract	4.0 $\pm$ 0.4	3.8 $\pm$ 0.3	4.7 $\pm$ 0.2	5.3 $\pm$ 0.9	11.2 $\pm$ 1.7

\*Based on region-of-interest (ROI) analysis of images in six patients with correction for radioactive decay and assuming that the whole-body counts immediately after injection of the radiopharmaceutical represents 100% of the injected dose.

**Table 4.** Pharmacokinetics of normal organ uptake of  $^{99m}\text{Tc}$ -hR3 following a 6 mg dose (1110 MBq). Results are given as the per cent injected dose/organ (mean  $\pm$  SEM).

Organ	Time post-injection				
	5–10 min	1–2 h	2–4 h	4–6 h	24 h
Heart	4.7 $\pm$ 0.4	3.3 $\pm$ 0.4	2.5 $\pm$ 0.3	2.4 $\pm$ 0.2	1.3 $\pm$ 0.1
Liver	44.0 $\pm$ 2.2	45.4 $\pm$ 2.3	35.5 $\pm$ 2.1	33.3 $\pm$ 2.2	20.9 $\pm$ 2.2
Kidneys	3.2 $\pm$ 0.3	3.7 $\pm$ 0.2	5.6 $\pm$ 0.7	7.2 $\pm$ 0.8	10.0 $\pm$ 1.1
Spleen	3.7 $\pm$ 0.4	2.9 $\pm$ 0.4	2.1 $\pm$ 0.2	2.0 $\pm$ 0.1	1.5 $\pm$ 0.1
Thyroid	0.26 $\pm$ 0.02	0.20 $\pm$ 0.02	0.19 $\pm$ 0.02	0.18 $\pm$ 0.02	0.13 $\pm$ 0.01
Gastrointestinal tract	2.4 $\pm$ 0.7	2.1 $\pm$ 0.5	2.6 $\pm$ 0.5	3.3 $\pm$ 0.3	9.3 $\pm$ 0.8

\*Based on region-of interest (ROI) analysis of images in six patients with correction for radioactive decay and assuming that the whole-body counts immediately after injection of the radiopharmaceutical represents 100% of the injected dose.

**Fig. 2.** Tomographic (A) sagittal and (B) coronal images of a patient with a squamous cell carcinoma of the floor of the mouth (Patient 5) at 3 h post-injection of  $^{99m}\text{Tc}$ -hR3 (3.0 mg, 938 MBq) demonstrating uptake of  $^{99m}\text{Tc}$  in involved cervical lymph nodes (arrow).

patient (Patient 3) had noticeable uptake of radioactivity in the right upper femur at 5 h, a site of metastasis previously identified on a whole-body bone scan. However, the intensity of activity at this site was not deemed to be sufficient for clear interpretation of malignancy. The remaining patients did not demonstrate tumour uptake of  $^{99m}\text{Tc}$ -hR3, although in four cases immunocytochemical staining of primary tumour biopsies demonstrated >50% EGFR positive cells (score >4) and the intensity of staining was moderate to strong (score 3–4).

#### Radiation dosimetry estimates

The radiation dosimetry estimates for  $^{99m}\text{Tc}$ -hR3 are shown in Table 5. The highest radiation absorbed doses were received by the kidneys ( $37.7 \pm 4.9 \times 10^{-8} \text{ mSv}\cdot\text{Bq}^{-1}$ ), spleen ( $38.6 \pm 4.5 \times 10^{-8} \text{ mSv}\cdot\text{Bq}^{-1}$ ) and gastrointestinal tract ( $30.0 \pm 4.3 \times 10^{-8} \text{ mSv}\cdot\text{Bq}^{-1}$ ). The radiation absorbed dose to the liver was  $6.6 \pm 0.8 \times 10^{-8} \text{ mSv}\cdot\text{Bq}^{-1}$ . The whole-body radiation absorbed dose was  $2.2 \pm 0.30 \times 10^{-8} \text{ mSv}\cdot\text{Bq}^{-1}$ .

#### Discussion

A significant proportion of epithelial malignancies over-express EGFR [2]. This feature is frequently associated with an aggressive phenotype and a poor prognosis. Several mAbs directed against EGFR have been developed in recent years and are being evaluated for treatment [12] and diagnosis [13] of epithelial derived malignancies. The murine anti-EGFR mAb ior egf/r3 has been tested in phase I/II trials as a diagnostic imaging tool [9] and also as a therapeutic agent [14]. The immunogenicity of murine mAbs in humans limits their clinical usefulness however, particularly if repeat administration is required [15]. The mAb hR3 is a humanized version of ior-R3 which has shown promise in animal tumour xenograft models for imaging EGFR positive malignancies [16]. In this report, we describe the results

**Table 5.** Radiation absorbed dose estimates in humans from the administration of  $^{99m}\text{Tc}$ -hR3.

Organ	Radiation absorbed dose ( $\text{mSv}\cdot\text{Bq}^{-1} \times 10^{-8}$ )*
Heart	$9.4 \pm 1.0$
Liver	$6.6 \pm 0.8$
Spleen	$38.6 \pm 4.5$
Kidneys	$37.7 \pm 4.9$
Gastrointestinal tract	$30.0 \pm 4.3$
Whole body	$2.2 \pm 0.3$

\*Mean  $\pm$  SEM.

of a phase I trial in 12 patients with epithelial derived tumours to evaluate the safety, pharmacokinetics, normal tissue biodistribution and radiation dosimetry of  $^{99m}\text{Tc}$ -hR3 as well as to obtain a preliminary assessment of its tumour imaging properties.

$^{99m}\text{Tc}$ -hR3 exhibited a good safety profile at doses up to 6.0 mg (1010 MBq, 27 mCi) as demonstrated by the absence of adverse effects, as well as biochemical parameters and peripheral blood cell counts which remained within the normal range. All patients exhibited WHO toxicity grade 0 before and after administration of  $^{99m}\text{Tc}$ -hR3.  $^{99m}\text{Tc}$ -hR3 was not immunogenic. There were no significant increases in HAMA or HAHA serum concentrations over a 4 week period following administration of the radiopharmaceutical. In contrast, about 20% of patients administered  $^{99m}\text{Tc}$ -ior-egf/r3 developed an immune response to the murine mAb [9]. The whole-body radiation absorbed dose from  $^{99m}\text{Tc}$ -hR3 ( $2.2 \pm 0.3 \times 10^{-8} \text{ mSv}\cdot\text{Bq}^{-1}$ ) was about 4-fold higher than that reported for  $^{99m}\text{Tc}$ -ior egf/r3 ( $4.7 \pm 0.5 \times 10^{-9} \text{ mSv}\cdot\text{Bq}^{-1}$ ), as a result of its longer whole-body mean residence time ( $4.9 \pm 0.7$  vs  $1.5 \pm 0.4$  h, respectively). In comparison to other nuclear medicine procedures, the whole-body radiation absorbed dose from  $^{99m}\text{Tc}$ -hR3 is higher than that for blood pool imaging using  $^{99m}\text{Tc}$  labelled red blood cells ( $0.4 \times 10^{-8} \text{ mSv}\cdot\text{Bq}^{-1}$ ) [17], but lower than that for tumour imaging using  $^{111}\text{In}$  satumomab pentetide mAb (Oncoscint<sup>®</sup>,  $15.0 \times 10^{-8} \text{ mSv}\cdot\text{Bq}^{-1}$ ) [18].

$^{99m}\text{Tc}$ -hR3 was rapidly cleared from the blood (Fig. 1) with a distribution phase half-life ( $T_d$ ) of  $10.8 \pm 3.8$  min (Table 2). The distribution half-life of  $^{99m}\text{Tc}$ -hR3 was similar to that reported for  $^{99m}\text{Tc}$ -ior egf/r3 in humans ( $8.2 \pm 4.6$  min) [19]. The volume of distribution ( $V_d$ ) for  $^{99m}\text{Tc}$ -hR3 was  $180.7 \pm 36.7 \text{ ml}\cdot\text{kg}^{-1}$ , approximately 4-fold higher than the expected plasma volume in humans ( $45 \text{ ml}\cdot\text{kg}^{-1}$ ) [20], but smaller than the  $V_d$  for  $^{99m}\text{Tc}$ -ior-egf/r3 ( $320.3 \pm 272.5 \text{ ml}\cdot\text{kg}^{-1}$ ) [19]. The rapid blood clearance and large  $V_d$  for  $^{99m}\text{Tc}$ -hR3 suggested sequestration of the radiopharmaceutical by normal organs. ROI analysis of images obtained immediately after injection revealed high accumulation of  $^{99m}\text{Tc}$  in the liver, and to a lesser extent in the kidneys and spleen. Liver and kidney uptake of the radiopharmaceutical were probably receptor mediated since these organs have moderate levels of EGFR expression which are about 10-fold higher than most normal epithelial tissues [21, 22].

The elimination phase of  $^{99m}\text{Tc}$ -hR3 from the blood or plasma could not be discerned due to an apparent increase in radioactivity (corrected for radioactive decay) at later time points (Fig. 1). We hypothesize that the increase in circulating radioactivity may be due

to catabolism of  $^{99m}\text{Tc}$ -hR3 in tissues such as the liver with subsequent appearance of  $^{99m}\text{Tc}$  catabolites in the blood.  $^{99m}\text{Tc}$ -hR3 was directly labelled by transchelation of  $^{99m}\text{Tc}$  (from  $^{99m}\text{Tc}$ -MDP) to free thiols generated in the antibody by mercaptoethanol reduction of disulfide bridges. This direct method of labelling antibodies with  $^{99m}\text{Tc}$  is commonly used due to its simplicity, high labelling efficiency and easy adaptability to kit formulation [23]. Antibodies labelled directly with  $^{99m}\text{Tc}$  through binding to thiols are relatively unstable *in vivo*, however, with gradual loss of  $^{99m}\text{Tc}$  to cysteine in the plasma or in tissues [24, 25]. Released  $^{99m}\text{Tc}$  bound to cysteine is excreted into the urine or via the hepatobiliary system into the gastrointestinal tract [25]. We did not determine the proportion of  $^{99m}\text{Tc}$  in the blood remaining bound to hR3 or present as catabolites, but ROI analysis of the images (Tables 3 and 4) clearly demonstrated a decrease in radioactivity in the liver over time, with an associated increase in kidney and gastrointestinal tract radioactivity. ROI analysis did not show an increase in thyroid radioactivity, which would suggest release of free [ $^{99m}\text{Tc}$ ]pertechnetate from  $^{99m}\text{Tc}$ -hR3. To improve the *in vivo* stability of  $^{99m}\text{Tc}$ -hR3, alternative methods of labelling could be considered including indirect labelling using diamidodithiol ( $\text{N}_2\text{S}_2$ ) chelates [26] or covalent binding of  $^{99m}\text{Tc}$  glucoheptonate to hydrazinicotinamide (HYNIC) functional groups introduced into the antibody [23]. The HYNIC method is the most easily adapted to kit formulation and provides similarly high labelling efficiencies for  $^{99m}\text{Tc}$ .

The main objectives in this phase I study were to evaluate the safety, pharmacokinetics, normal tissue biodistribution and radiation dosimetry of  $^{99m}\text{Tc}$ -hR3. Nevertheless, tumour localization was noted in one patient. In this patient (Patient 5), a positive image was obtained of a squamous cell carcinoma of the floor of the mouth and an involved cervical lymph node. Although immunocytochemical staining of the primary tumour biopsy from Patient 5 was highly positive for EGFR expression, in most instances EGFR positivity in the primary malignancy was not correlated with positive tumour imaging of metastases using  $^{99m}\text{Tc}$ -hR3. Possible explanations for this discordant result include differences in epitope recognition between the 31G7 murine mAb used for the immunocytochemical staining and the hR3 antibody used for imaging; differences in EGFR expression between the primary tumour and metastases; and the qualitative nature of immunocytochemical staining. The sensitivity of tumour imaging is more dependent on the quantitative level of EGFR expression on cancer cells than on a qualitative measure such as EGFR positivity/negativity [27]. In order to address this issue, both the intensity and heterogeneity of EGFR staining

in the tumour biopsies were scored to provide semi-quantitative information, but this proved insufficient to predict positive tumour imaging with  $^{99m}\text{Tc}$ -hR3. Interestingly, immunocytochemical staining of tumour biopsies for c-erbB2 (HER-2/neu) has also not proven a reliable indicator of c-erbB2 gene amplification in breast cancer, with a false positive rate of 17–23% [28]. Fluorescence *in situ* hybridization (FISH) has recently been recommended as an alternative to immunocytochemical staining for selecting patients for treatment with anti-c-erbB2 mAb trastuzumab (Herceptin<sup>®</sup>) [28]. A quantitative measure of EGFR expression in tumour biopsies (e.g. radioimmunoassay) with a clinically relevant cut-off value [29] may be helpful in pre-selecting patients for tumour imaging with  $^{99m}\text{Tc}$ -hR3.

In addition to the level of receptor expression on cancer cells, numerous other factors can affect tumour imaging with receptor binding radiopharmaceuticals, including the level of radiopharmaceutical uptake in the tumour nodule, the extent of normal organ sequestration, the tumour/background ratio, as well as attenuation of the tumour signal by overlying tissues [27]. The liver accumulated 44–49% of the injected dose of  $^{99m}\text{Tc}$ -hR3 (Tables 3 and 4) which significantly diminished the proportion of antibody molecules available for binding to EGFR positive cancer cells. In a phase I trial of anti-EGFR mAb C225 in 19 patients with squamous cell carcinoma of the lung, high liver accumulation was also observed [30]. However, by increasing the administered mass of  $^{111}\text{In}$ -C225 from 40 mg to 300 mg, liver sequestration was decreased by almost one third (from 32% to 22% of the injected dose). Increasing the mass of  $^{111}\text{In}$ -C225 also significantly increased the plasma half-life of the antibody from 42 min at a dose of 4 mg, to 13.9 h at a dose of 40 mg, and to 49.5 h at a dose of 300 mg. Tumour imaging was positive in all known lesions using a dose of  $\geq 40$  mg of  $^{111}\text{In}$ -C225, but at a dose of 4 mg, only 3/5 primary lesions and 0/5 metastases were detected. One method of improving the sensitivity for tumour imaging with  $^{99m}\text{Tc}$ -hR3 may therefore be to increase the mass of the antibody administered. In this phase I study, the mass of  $^{99m}\text{Tc}$ -hR3 was modestly increased from 3.0 mg in the first group of six patients, to 6.0 mg in the second six patients, but this did not significantly diminish hepatic uptake. The experience with  $^{111}\text{In}$ -C225 suggests that much higher doses ( $\geq 40$  mg) of  $^{99m}\text{Tc}$ -hR3 may be required to decrease liver uptake and promote tumour localization. The safety of administration of these doses of  $^{99m}\text{Tc}$ -hR3 to humans is not currently known, but mAb *ior egf/r3* has been safely administered in doses ranging from 50 mg to 500 mg in a phase I trial in 19 patients with epithelial tumours. There was only a single case of a serious side effect (hypotension and lethargy) [14].

## Conclusion

We conclude that <sup>99m</sup>Tc-hR3, a humanized analogue of the murine anti-EGFR mAb ior egf/r3 is safe to administer to humans at doses up to 6.0 mg (1010 MBq, 27 mCi). The radiopharmaceutical was rapidly cleared from the blood after injection localizing mainly in the liver, kidneys and spleen. Immunocytochemical staining of primary tumour biopsies for EGFR positivity did not predict positive tumour imaging in most cases. Nevertheless, one positive image was obtained. High accumulation in the liver and metabolism restrict the proportion of <sup>99m</sup>Tc-hR3 molecules available for binding to EGFR positive tumour cells. Improvements in the sensitivity of tumour imaging with <sup>99m</sup>Tc-hR3 could potentially be achieved by increasing the mass of administered antibody to decrease liver sequestration, and by using more stable <sup>99m</sup>Tc labelling methods. Future studies in a larger group of patients with epithelial malignancies or in patients with a single type of cancer, with pre-screening for tumour EGFR positivity are planned to more accurately define the sensitivity and specificity of <sup>99m</sup>Tc-hR3 for tumour imaging.

## Acknowledgements

The authors wish to thank Martha Maclean, clinical trials nurse and Wendy Denovan and Julie Mathewson, nuclear medicine technologists at the University Health Network for their assistance with this study. The study was financially supported by a grant from YM Biosciences Inc.

## References

1. Kwekkeboom DJ, Krenning EP, de Jong M. Peptide receptor imaging and therapy. *J Nucl Med* 2000; **41**: 1704–1713.
2. Gullick WJ. Prevalence of aberrant expression of the epidermal growth factor receptor in human cancers. *Br Med Bull* 1991; **47**: 87–98.
3. Sirotiak FM, Zakowski MF, Miller VA, Scher HI, Kris MG. Efficacy of cytotoxic agents against human tumor xenografts is markedly enhanced by coadministration of ZD1839 (Iressa), an inhibitor of EGFR tyrosine kinase. *Clin Cancer Res* 2000; **6**: 4885–4892.
4. Baselga J, Pfister D, Cooper MR, *et al.* Phase I studies of anti-epidermal growth factor receptor chimeric antibody C225 alone and in combination with cisplatin. *J Clin Oncol* 2000; **18**: 904–914.
5. Arteaga CL, Hurd SD, Dugger TC, Winnier AR, Robertson JB. Epidermal growth factor receptors in human breast carcinoma cells: a potential selective target for transforming growth factor  $\alpha$ -*Pseudomonas* exotoxin 40 fusion protein. *Cancer Res* 1994; **54**: 4703–4709.
6. Heimbrook DC, Stirdivant SM, Ahern JD, *et al.* Transforming growth factor  $\alpha$ -*Pseudomonas* exotoxin fusion protein prolongs survival of nude mice bearing tumor xenografts. *Proc Natl Acad Sci USA* 1990; **87**: 4697–4701.
7. Reilly RM, Kiarash R, Cameron RG, *et al.* <sup>111</sup>In-labeled EGF is selectively radiotoxic to human breast cancer cells overexpressing the EGFR. *J Nucl Med* 2000; **41**: 429–438.
8. Fernandez A, Spitzer E, Perez R, *et al.* A new monoclonal antibody for detection of EGF receptors in western blots and paraffin-embedded tissue sections. *J Cell Biochem* 1992; **49**: 157–165.
9. Ramos-Suzarte M, Rodriguez N, Oliva JP, *et al.* <sup>99m</sup>Tc-labeled antihuman epidermal growth factor receptor antibody in patients with tumors of epithelial origin: Part III. Clinical trials safety and diagnostic efficacy. *J Nucl Med* 1999; **40**: 768–775.
10. Mateo C, Moreno E, Amour K, Lombardero J, Harris W, Perez R. Humanization of a mouse monoclonal antibody that blocks the epidermal growth factor receptor: recovery of antagonistic activity. *Immunotechnol* 1997; **3**: 71–81.
11. Watson EE, Stabin M, Bolch WE. MIRDOSE Ver 3.0 (computer program). Oak Ridge, TN: Oak Ridge Associated Universities, 1994.
12. Ciardiello F, Tortora G. A novel approach in the treatment of cancer: targeting the epidermal growth factor receptor. *Clin Cancer Res* 2001; **7**: 2958–2970.
13. Reilly RM, Kiarash R, Sandhu J, *et al.* A comparison of EGF and MAb 528 labeled with <sup>111</sup>In for imaging human breast cancer. *J Nucl Med* 2000; **41**: 903–911.
14. Crombet T, Torres O, Neninger E, *et al.* Phase I clinical evaluation of a neutralizing monoclonal antibody against epidermal growth factor receptor. *Cancer Biother Radiopharm* 2001; **16**: 93–102.
15. Reilly RM, Sandhu J, Alvarez-Diez TM, Gallinger S, Kirsh J, Stern H. Problems of delivery of monoclonal antibodies. Pharmaceutical and pharmacokinetic solutions. *Clin Pharmacokinet* 1995; **28**: 126–142.
16. Morales AA, Duconge J, Alvarez-Ruiz D, *et al.* Humanized versus murine anti-human epidermal growth factor receptor monoclonal antibodies for immunoscintigraphic studies. *Nucl Med Biol* 2000; **27**: 199–206.
17. Technescan PYP®. Kit for the preparation of technetium Tc-99m pyrophosphate injection. St. Louis, MO: Mallinckrodt Medical Inc., 2000.
18. Oncoscint® CR/OV Kit (satumomab pendetide) for the preparation of indium-111 satumomab pendetide. Princeton, NJ: Cytogen Corp., 1996.
19. Iznaga-Escobar N, Torres Arocha LA, Morales Morales A, Ramos Suzarte M, Rodriguez Mesa N, Perez Rodriguez R. Technetium-99m-antiepidermal growth factor-receptor antibody in patients with tumors of epithelial origin: part II. Pharmacokinetics and clearances. *J Nucl Med* 1998; **39**: 1918–1927.
20. Elin RJ. Laboratory reference intervals and values. In: J.C. Bennett, F. Plum, eds. Cecil textbook of medicine. Philadelphia, PA: Saunders, 1996: 2230.

21. Dunn WA, Hubbard AL. Receptor-mediated endocytosis of epidermal growth factor by hepatocytes in the perfused rat liver: ligand and receptor dynamics. *J Cell Biol* 1984; **98**: 2148–2159.
22. Fisher DA, Salido EC, Barajas L. Epidermal growth factor and the kidney. *Annu Rev Physiol* 1989; **51**: 67–80.
23. Schwartz DA, Abrams MJ, Hauser MM, et al. Preparation of hydrazino-modified proteins and their use for the synthesis of  $^{99m}\text{Tc}$ -protein conjugates. *Bioconjugate Chem* 1991; **2**: 333–338.
24. Mardirosian G, Wu C, Rusckowski M, Hnatowich DJ. The stability of  $^{99}\text{Tc}^m$  directly labelled to an Fab' antibody via stannous ion and mercaptoethanol reduction. *Nucl Med Commun* 1992; **13**: 503–512.
25. Reilly RM. Immunoscintigraphy of tumours using  $^{99}\text{Tc}^m$ -labelled monoclonal antibodies: a review. *Nucl Med Commun* 1993; **14**: 347–359.
26. Fritzberg AR, Abrams PG, Beaumier PL, et al. Specific and stable labeling of antibodies with technetium-99m with a diamide dithiolate chelating agent. *Proc Natl Acad Sci* 1988; **85**: 4025–4029.
27. Reilly RM, Gariépy J. Factors influencing the sensitivity of tumour imaging with a receptor-binding radiopharmaceutical. *J Nucl Med* 1998; **39**: 1036–1043.
28. Tubbs RR, Pettay JD, Roche PC, Stoler MH, Jenkins RB, Grogan TM. Discrepancies in clinical laboratory testing of eligibility for trastuzumab therapy: apparent immunohistochemical false-positives do not get the message. *J Clin Oncol* 2001; **19**: 2714–2721.
29. Nicholson S, Sainsbury JRC, Needham GK, Chambers P, Farndon JR, Harris AL. Quantitative assays of epidermal growth factor receptor in human breast cancer: cut-off points of clinical relevance. *Int J Cancer* 1988; **42**: 36–41.
30. Divgi CR, Welt S, Kris M, et al. Phase I and imaging trial of indium 111-labeled anti-epidermal growth factor receptor monoclonal antibody 225 in patients with squamous cell lung carcinoma. *J Natl Cancer Inst* 1991; **83**: 97–104.